Improvement in elevated-temperature properties of Al-13%Si piston alloys by dispersoid strengthening via Mn addition

K. Liu*, X.-G. Chen

Department of Applied Sciences, University of Quebec at Chicoutimi,
Saguenay, (Quebec), Canada, G7H 2B1

*Corresponding author: kun.liu @uqac.ca; Tel.: 1-4185455011 ext.7112; Fax: 1-4185455012

Abstract

Eutectic Al-13%Si alloys are widely used in automotive components, such as pistons and cylinder heads. Recently, the demand on the performance of piston alloys at high temperature is greatly increased to enhance the engine efficiency and to reduce exhaust emission. In the present work, Mn was added to strengthen the aluminum matrix via the formation of thermally stable dispersoids. The evolution of dispersoids during heat treatment and their influence on elevated-temperature properties were studied. Results show that the as-cast microstructures in the experimental alloys without/with Mn addition were similar, which was composed of eutectic Si, primary Mg_2Si, Al-Fe-Ni, Al-Cu-Ni and π-Al-Mg-Fe-Si intermetallic phases. In the alloy with Mn addition, a number of α-Al(Mn,Fe)Si dispersoids started to form after heat treatment at 425 °C for 24 h and reached the peak condition at 500 °C for 6 h, resulting in a remarkable increase of the microhardness at room temperature and the improvement in the yield strength and creep resistance at 300 °C. As a complementary strengthening mechanism, the dispersoid strengthening in the aluminum matrix provides a novel approach to improve the elevated-temperature properties of Al-Si piston alloys.

Keywords: Al-Si piston alloys; Dispersoids; Mn; elevate-temperature properties.

1. Introduction

Due to the high strength, excellent wear resistance and low thermal expansion, eutectic Al-13%Si piston alloys (all alloy composition in the present work is in wt.% unless indicated otherwise) are widely used as automobile components, such as pistons and cylinder heads [1, 2]. In recent years, the increasing demands in the legislation about exhaust emissions place higher requirement on the performance of materials, especially at elevated temperature, such as 250-350 °C [3]. Therefore, how to improve the elevated-temperature properties of piston alloys is becoming the significant concern in industries.

Up to date, the enhancement of elevated-temperature properties of Al-Si piston alloys are principally derived from the addition of alloying elements (i.e. Fe and Ni) to form a large volume fraction of various intermetallics during solidification [4-9], which can establish the three-dimensional rigid networks with Si particles [9]. For instance, the elevated temperature properties of an Al-12%Si alloy was improved by addition of 2% Ni, while the combined addition of Ni and Fe could further improve the elevated-temperature properties by forming the Al-Fe-Ni aluminides [10]. In addition, the transition alloying elements, such as Cr, Zr and V, were also reported to benefit the elevated-temperature properties of Al-Si alloys by formation of various intermetallics [7, 9]. In the above cited studies, all the various intermetallics are formed in the interdendrite regions and grain boundaries to form the 3-D rigid networks and then enhance the elevated-temperature properties. However, the networks can be weakened during the solution treatment and after long-time service at elevated temperatures, especially the fragmentation of Si particles [6, 11]. Very little literature can be found on strengthening the aluminum matrix to improve their elevated-temperature properties of Al-Si piston alloys. Recently, the dispersoid strengthening is found to be an efficient way to improve the elevated-temperature properties by forming the thermally stable dispersoids in the aluminum matrix [12-14], providing the potential avenue to further improve the elevated-temperature properties of Al-Si piston alloys.

In the present work, the formation of dispersoids by the Mn addition (0.5%) in an Al-13%Si piston alloy was studied by characterizing the dispersoids during various heat treatments. The influence of dispersoids on the yield strength and creep resistance at 300 °C was investigated. The appropriate heat treatment for dispersoid precipitation which is compatible to conventional T6/T7 heat treatment of Al-Si piston alloys was discussed.

2. Experimental

Two Al-13%Si alloys were prepared in the present work; Alloy A was the base 13%Si alloy while 0.5% Mn was added in the base alloy to form Alloy M5. For other alloying elements, such as Fe, Ni, Cu and Mg, they were the same in both alloys and designed according to the literature [5]. The chemical compositions of experimental alloys analyzed with an optical emission spectrometer are listed in Table I.

Table I Chemical composition of experimental alloys (wt.%)

In each test, approximately 3 kg of materials was prepared in a clay-graphite crucible using an electric resistance furnace. The temperature of the melt was maintained at ~750 °C for 30 min. An Al-3.5%P master alloy was added to modify the Si particles.

The melt was degassed for 15 min and then poured into a permanent mold preheated at 250 °C. The dimension of the cast ingots was 30 mm×40 mm×80 mm.

After casting, the heat treatment was carried out at 375 °C, 425 °C and 500 °C with various holding times up to 24 hours followed by water quenching. The precipitation behavior of dispersoids after heat treatments was evaluated by electrical conductivity (EC) and Vickers microhardness at room temperature (RT) as well as the compression yield strength (YS) and creep resistance at 300 °C. EC was recorded as an average value of 5 measurements. Microhardness tests were performed with a load of 200 g and a dwell time of 20 s on polished samples. The locations of indentations were on the aluminum matrix to determine the influence of dispersoids rather than the intermetallics on the boundaries. The average value of 20 measurements was recorded for each sample. The YS at 300 °C was obtained from compression tests with the strain rate of 10^{-3} s^{-1}. In addition, creep tests at 300 °C were also performed under compression with a constant load of 45 MPa. For each condition, 3 tests were repeated to confirm the reliability of the results. More details of experiments can be found in the literatures [13, 14]. All the compression tests and creep tests were performed after the samples were hold at 300 °C for 100 hours to remove the influence of aging effect of experimental alloys [8, 15].

The microstructural features of experimental alloys were observed by optical and electron microscopes. The intermetallics were characterized by a scanning electron microscope (SEM, JSM-6480LV) equipped with an energy dispersive x-ray spectrometer (EDS) and by X-ray diffraction (XRD). To reveal the dispersoids clearly, the polished samples were etched in 0.5% HF for 30 seconds. In addition, the dark-field mode on the optical microscope (OM) was used to observe the fine dispersoids. A transmission electron microscope (TEM, JEM-2100) operated at 200kV was used to observe the distribution of dispersoids in details.

3. Results and Discussion

3.1 As-cast microstructure of experimental alloys

Fig. 1 shows the as-cast microstructure of two experimental alloys. It can be seen that the formed phases are similar in both Alloy A and Alloy M5, which are composed of dark gray eutectic Si, dark primary Mg_2Si, gray π-Al-Mg-Fe-Si phase ($Al_8Mg_3FeSi_6$), light gray Al-Fe-Ni and bright Al-Cu-Ni phases [4, 5]. The micro-constituents of two experimental alloys were also confirmed by the XRD results (Fig. 2), in which the peaks of six different phases (including Al matrix, Si, Mg_2Si, Al-Cu-Ni, Al-Fe-Ni and π-phase) were detected with similar intensities [5]. A few of α-Al(MnFe)Si intermetallic particles were occasionally observed in Alloy M5 (not shown in Fig. 1b). However, their volume fraction is very low and they are not detected by XRD in Fig. 2.

Fig. 1 Backscatter SEM images showing as-cast microstructure of experimental alloys: (a) Alloy A and (b) Alloy M5

Fig. 2 XRD results of two experimental alloys in as-cast condition

As shown in Figs. 1 and 2, no new intermetallic phase is observed in Alloy M5 compared with Alloy A, indicating that most of Mn remained in the aluminum matrix after the solidification due to its high solubility in Al [16]. This is also indirectly confirmed by the EC and microhardness data of two alloys at as-cast condition, which is measured to be 33.7 and 29.7 %IACS, 75.6 and 81.6 HV in Alloy A and Alloy M5, respectively. The lower EC and higher microhardness in Alloy M5 can be contributed to the solid solution strengthening of Mn.

3.2 Evolution of dispersoids during heat treatment

In the present work, EC and microhardness were measured after various heat treatments performed at 375 °C, 425 °C and 500 °C to investigate the precipitation behavior of dispersoids. Figs. 3a-b shows the evolution of EC and microhardness as a function of the holding time at 375 °C. The EC keeps rising with the time up to 8 hours (Fig. 3a), while the microhardness decreases up to 8 hours followed by a plateau. The tendency of EC and microhardness changes in both alloys is similar. The differences of EC and microhardness between two alloys are derived by the solute Mn in the aluminum matrix.

Fig. 3 Evolution of EC and microhardness: (a) EC and (b) microhardness during heat treatment at 375 °C; (c) EC and (d) microhardness during heat treatment at 425 °C

The microstructure after 375°C/24h of both alloys is shown in Fig. 4. It can be observed that a number of small dark particles appeared in the core of aluminum dendrites in both alloys (Figs. 4a and 4b). Fig. 4c and 4d shows the SEM images of these small particles, which have the same morphology and are identified to be β-Mg_2Si by SEM-EDS results, which was also reported to precipitate at ~ 400 °C in Al-Si piston alloys [17]. The continuous precipitation of equilibrium β-Mg_2Si phase from the aluminum matrix leads to the increase of EC [18]. However, due to the large size (~ 500 nm) and low volume fraction of Mg_2Si, their contribution to the hardness is weaker than the solid solution effect if they are present as the solute Mg and Si in the matrix [13], resulting in the decrease of microhardness (Fig. 3b). No Mn-containing dispersoids were observed at this condition although it was reported that the α-Al(Mn,Fe)Si dispersoids could precipitate at 375 °C and reached the peak condition after 24-48 hours at 375 °C in Al-Mn-Mg 3004 alloys [13]. The reason is unclear but it is likely contributed to a much higher silicon (13%) in the experimental alloys than that in 3004 alloy (0.25% Si), which was reported that the precipitation temperature of dispersoids increased with increasing Si content [18].

Fig. 4 Optical (a-b) and SEM (c-d) observation on the microstructure after 375°C/24h: (a) and (c) for Alloy A, (b) and (d) for Alloy M5

With increasing the heat treatment temperature from 375 °C to 425 °C, the similar tendency of EC and microhardness changes is observed, which is shown in Figs. 3c-d. The EC increases while microhardness decreases with holding time up to 10 hours followed by a plateau (Fig. 3c), which is resulted from the precipitation of equilibrium β-Mg_2Si from the matrix. However, a slight decrease in EC and a moderate increase in microhardness are observed after 10 hours, which can be attributed to the dissolution of Mg_2Si particles back in the matrix [14, 18]. As shown in Fig. 5a, only large Mg_2Si particles remained in aluminum dendrites while small Mg_2Si particles dissolved back to aluminum matrix. On the other hand, the difference in microhardness after 425°C/24h becomes bigger between two alloys (Fig. 3d), suggesting the possible decomposition of Mn supersaturated solution and formation of Mn-containing dispersoids. As shown in Fig. 5b, a number of fine dispersoids appeared in aluminum matrix in addition to large Mg_2Si particles in Alloy M5 after 425°C/24h, making an additional contribution to the microhardness in Fig. 3d. However, the volume fraction of dispersoids is low with high volume fraction of dispersoid free zone, resulting in a limited contribution to the increase of microhardness in Alloy M5 after 425°C/24h.

Fig. 5 Dark-field OM microstructure of experimental alloys after 425°C/24h: (a) Alloy A and (b) Alloy M5

With further increasing heat treatment temperature to 500 °C, both the EC and microhardness generally increase with increasing time in both alloys (Fig. 6). However, significant difference can be observed between Alloy A and Alloy M5. As shown in Fig. 6a, there is a sharp increase in EC in Alloy M5 at first few hour holding and the difference in EC after 6h holding between two alloys is much smaller at 500°C compared with 375 °C and 425 °C (Fig. 3). As shown in Fig. 5, most of Mg_2Si particles have been dissolved into the aluminum matrix at 425 °C for 24 h. Therefore, the sharper increasing EC in Alloy M50 than Alloy A is likely resulted from the rapid decomposition of supersaturated solid solution of Mn in the matrix, while the slight increase of EC in Alloy A is likely due to the fragmentation of Si particles [19], which is also shown in Figs. 7a and b. In addition, it can be found that the EC of both alloys is very close after 12 h at 500 °C, indicating the full decomposition of Mn supersaturated solid solution. For the evolution of microhardness at 500 °C (Fig. 6b), the difference in microhardness between Alloy M5 and Alloy A becomes bigger and the microhardness reaches the peak value after 6 h followed by a slightly decrease until to 24 h. For instance, the difference in microhardness between two alloys is around 6 HV at as-cast condition due to the solid solution of Mn in the matrix. However, it increases to maximum 15 HV at 500°C/6h and remains 10 HV at 500°C/24h, indicating the optimum condition can be obtained at

500°C/6h in Alloy M5 due to the full decomposition of Mn supersaturated solid solution and the precipitation of dispersoids.

Fig. 6 Evolution of EC and microhardness during heat treatment at 500 °C: (a) EC and (b) microhardness

Fig. 7 shows the microstructure of Alloys B and M5 after 500°C/6h and 500°C/24h after etching. As shown in Figs. 7a and b, the matrix of Alloy B is very clear with little particles in the dendrite cells after both 6 and 24 hours holding. On the other hand, the fine dispersoid zones can be clearly observed in Alloy M5 after 500°C/6h (Fig. 7c), in which a large number of dispersoids are uniformly distributed in the dendrite cells with surrounding narrow dispersoid free zones. With increasing time (24 hours in Fig. 7d), the dispersoids are still uniformly distributed. However, their size becomes larger and the dispersoid free zone becomes bigger. Therefore, the precipitation of high volume and fine dispersoids at 500°C/6h makes a significant contribution to the hardness, leading to the peak value at 500°C/6h in Fig. 6b. With further increasing holding time, the microhardness slightly decreases due to the increasing size of dispersoids and the increasing volume of dispersoid free zones.

Fig. 7 Dark-field OM microstructure of experimetal alloys after treated at 500 °C: (a) Alloy A: 6h and (b) Alloy A: 24h; (c) Alloy M5: 6h and (d) Alloy M5: 24h

In order to characterize the dispersoids in the details, TEM observation is performed in the disepersoid zone in Alloy M5. Though the morphology of dispersoids is slightly different (Fig. 8a and b), all the dispersoids are confirmed as Mn-containing dispersoids from TEM-EDS results (Fig. 8c), which is similar to the composition of α-Al(Mn,Fe)Si dispersoids reported in the literatures [12, 13, 18]. The dispersoids after heat treatment at 500°C/6h are uniformly distributed in the matrix with the average diameter of ~ 90 nm (Fig. 8a) and with the number density as high as 8×10^{12} m^{-2}, confirming their remarkable contribution to the microhardness in Fig. 7. However, with increasing time (500°C/24h in Fig. 8b), the size of α-Al(Mn,Fe)Si dispersoids become larger with the average diameter of ~ 150 nm and their number density becomes much lower (2.5×10^{12} m^{-2}) compared with that in 500°C/6h, indicating the coarsening of α-dispersoids that causes a slight decrease of microhardness after 6 hours in Fig. 6.

Fig. 8 TEM images showing the distribution of dispersoids in Alloy M5: (a) 500°C/6h, (b) 500°C/24h and (c) their TEM-EDS result

3.3 Elevated-temperature properties of experimental alloys

As shown in Figs. 4 and 5, though the Mg_2Si particles could precipitate in aluminum matrix during heat treatment at lower temperatures (375 – 425 °C), their contribution to the microhardness is limited due to the large size and low volume fraction (Figs. 4a and 5a), and often is negative due to the weaker hardening effect than the solid solution strengthening of solute Mg and Si in the matrix, leading to the decreasing microhardness (Figs. 3b and 3d). On the other hand, the Mn-containing α-Al(Mn,Fe)Si dispersoids precipitated during heat treatment at higher temperature (~500 °C) with fine size and relatively high number density (Fig. 8a), leading to a remarkable contribution to the microhardness at room temperature (Fig. 6b). For the elevated-temperature properties, the YS and creep resistance at 300 °C were measured with samples treated at 500 °C followed by holding at 300 °C for 100 hours. The results obtained from two experimental alloys are shown in Fig. 9.

Fig. 9 Evolution of properties at 300 °C of experimental alloys :
(a) YS as a function of holding time at 500 °C and
(b) typical creep curves after 500°C/6h, tested under with a constant load of 45 MPa

As shown in Fig. 9a, different tendency of YS at 300 °C between Alloy A and Alloy M5 can be observed. For Alloy A, the YS begins to decrease after 6 hours, which is likely due to a loss of interconnectivity of the networks between Si particles and intermetallic particles caused by the fragmentation and spheroidization of eutectic Si particles with increasing holding time at 500 °C [6, 11]. On the other hand, the YS at 300 °C in Alloy M5 firstly increases to the peak value after 6 hours followed by a slight decrease with time. As shown in Figs. 7c and 8a, fine Mn-containing dispersoids have fully precipitated after 500°C/6h, which is the main reason for the increase of YS at 300 °C due to the dispersoid hardening according to the Orowan strengthening mechanism [13, 20] . As shown in Fig. 9a, the peak YS at 300 °C is improved from 63 MPa in Alloy A to 74 MPa in Alloy M5 after 500°C/6h, which is 17.5% improvement in the elevated-temperature strength. For the decrease of YS after 6 hours in Alloy M5, two mechanisms can be involved: coarsening of Mn-containing dispersoids and weakening of internal networks between Si particles and intermetallic particles. Although the YS decreases with time after 6 hours in Alloy M5, their values at 300 °C are always higher than Alloy A. For instance, the YS of Alloy M5 after 500°C/24h is still as high as 64 MPa, which is almost 9 MPa higher than that of Alloy A (55 MPa after 500°C/24h), confirming the remarkable contribution of dispersoids on the elevated-temperature strength.

Fig. 9b is the typical creep curves of Alloys A and M5 after treated 500°C/6h. For Alloy A, it took around 50 hours to reach the maximum creep strain of 0.25, which is the limitation of the creep testing machine. However, it took more than 85 hours to reach the creep strain of 0.25, indicating the better creep resistance of Alloy M5 at elevated temperature. Due to the creep condition applied in the present work (300 °C, 45 MPa), the creep deformation was principally controlled by the dislocation mechanism [13]. Therefore, the precipitation of dispersoids in Alloy M5 can be the principal reason for the improvement in the creep resistance.

From the evolution of microhardness at room temperature (Fig. 7) and the yield strength and creep resistance at 300 °C (Fig. 10), it can be concluded that the properties at both room and elevated temperatures can be optimized in Alloy M5 after 500°C/6h due to the precipitation of a high volume of α-Al(Mn,Fe)Si dispersoids (Fig. 9). In the industrial practice, the Al-Si piston alloys are subjected an artificial aging after solution treatment (T6 and T7) to enhance the room temperature mechanical properties. Conventionally, the artificial aging treatment is performed at relative low temperature (160-200 °C) to form the fine precipitates as the main strengthening phases, such as Mg2Si, Al2Cu and Al2CuMg [8, 21]. In the present work, the α-Al(Mn,Fe)Si dispersoids are precipitated during the solution treatment at higher temperature (~500 °C). After the solution treatment and quench, Mg and Cu solutes are supersaturated in the aluminum matrix, which are ready to form the fine precipitates during the artificial aging. On the other hand, the formation of α-Al(Mn,Fe)Si dispersoids does not consume any Mg and Cu solutes. Therefore, it is expected that the precipitation of α-Al(Mn,Fe)Si dispersoids during the solution treatment has little influence on the subsequent aging behavior. The heat treatment of the dispersoid precipitation at 500 °C in the present work is completely compatible to the conventional heat treatments (T6 and T7) in Al-Si piston alloys. When the piston alloys are exposed to the working condition at elevated temperature, the fine precipitates obtained by aging become coarsening and the mechanical properties drop. As a complementary strengthening mechanism, the dispersoid strengthening in the aluminum matrix provides an alternative approach to improve both the room-temperature and elevated-temperature properties for Al-Si based piston alloys, especially due to their thermal stability of the dispersoids at elevated temperature.

4. Conclusions

In the present work, the influence of Mn addition on the evolution of dispersoids and elevated-temperature properties was investigated and the following conclusions can be obtained:

(1) No obvious changes on the as-cast microstructure are observed in the alloy with Mn addition, which is composed of eutectic Si, primary Mg_2Si, Al-Fe-Ni, Al-Cu-Ni, π-Al-Mg-Fe-Si intermetallic phases.

(2) During the heat treatment at low temperature (~375 °C), β-Mg_2Si particles can precipitate in the matrix. However, their contribution to microhardness is negative due to the large size and low number density, resulting in a weaker strengthening effect than solid solution hardening of solute Mg and Si atoms. Almost all the Mg_2Si particles can be dissolved in the aluminum matrix at 500 °C.

(3) α-Al(Mn,Fe)Si dispersoids begin to form at 425 °C for 24 hours and the full precipitation of dispersoids reaches at 500 °C for 6 hours, resulting in a remarkable improvement in the microhardness at room temperature and the yield strength and the creep resistance at 300 °C.

(4) The heat treatment of the dispersoid precipitation (500°C/6h) in Al-Si piston alloys with Mn addition is completely compatible with the convention heat treatments (T6 and T7), providing an alternative approach to improve both the room-temperature and elevated-temperature properties of Al-Si piston alloys.

Acknowledgments

The authors would like to acknowledge the financial support of the Natural Sciences and Engineering Research Council of Canada (NSERC) and Rio Tinto Aluminum through the NSERC Industry Research Chair in the Metallurgy of Aluminum Transformation at University of Québec at Chicoutimi.

References

[1] M. M. Haque, A. Sharif Study on wear properties of aluminium–silicon piston alloy. J. Mater. Process. Technol. , 118, 69 (2001).
[2] N. A. Belov, D. G. Eskin, N. N. Avxentieva Constituent phase diagrams of the Al–Cu–Fe–Mg–Ni–Si system and their application to the analysis of aluminium piston alloys. Acta Materialia, 53, 4709 (2005).
[3] M. R. Joyce, C. M. Styles, P. A. S. Reed Elevated temperature short crack fatigue behaviour in near eutectic Al-Si alloys. Int. J. Fatigue 25, 863 (2003).
[4] Z. Asghar, G. Requena, F. Kubel The role of Ni and Fe aluminides on the elevated temperature strength of an AlSi12 alloy. Mater. Sci. Eng., A, 527, 5691 (2010).
[5] Y. Li, Y. Yang, Y. Wu, L. Wang, X. Liu Quantitative comparison of three Ni-containing phases to the elevated-temperature properties of Al–Si piston alloys. Mater. Sci. Eng., A, 527, 7132 (2010).
[6] Z. Asghar, G. Requena, E. Boller Three-dimensional rigid multiphase networks providing high-temperature strength to cast AlSi10Cu5Ni1-2 piston alloys. Acta Mater. , 59, 6420 (2011).
[7] Y. Li, Y. Yang, Y. Wu, Z. Wei, X. Liu Supportive strengthening role of Cr-rich phase on Al–Si multicomponent piston alloy at elevated temperature. Mater. Sci. Eng., A, 528, 4427 (2011).
[8] E. R. Wang, X. D. Hui, G. L. Chen Eutectic Al–Si–Cu–Fe–Mn alloys with enhanced mechanical properties at room and elevated temperature. Mater. Des., 32, 4333 (2011).
[9] M. Zamani, L. Morini, L. Ceschini, S. Seifeddine The role of transition metal additions on the ambient and elevated temperature properties of Al-Si alloys. Mater. Sci. Eng., A, 693, 42 (2017).

[10] Z. Asghar, G. Requena, H. P. Degischer, P. Cloetens Three-dimensional study of Ni aluminides in an AlSi12 alloy by means of light optical and synchrotron microtomography. Acta Mater. , 57, 4125 (2009).
[11] W. Eidhed Effect of solution treatment time and Sr-modification on microstructure and mechanical property of Al-Si piston alloy. J. Mater. Sci. Technol., 24, 29 (2008).
[12] Y. J. Li, A. M. F. Muggerud, A. Olsen, T. Furu Precipitation of partially coherent α-Al(Mn,Fe)Si dispersoids and their strengthening effect in AA 3003 alloy. Acta Mater., 60, 1004 (2012).
[13] K. Liu, X. G. Chen Development of Al–Mn–Mg 3004 alloy for applications at elevated temperature via dispersoid strengthening. Mater. Des., 84, 340 (2015).
[14] K. Liu, H. Ma, X. G. Chen Enhanced elevated-temperature properties via Mo addition in Al-Mn-Mg 3004 alloy. J. Alloys Compd. , 694, 354 (2017).
[15] Z. Qian, X. Liu, D. Zhao, G. Zhang Effects of trace Mn addition on the elevated temperature tensile strength and microstructure of a low-iron Al–Si piston alloy. Mater. Lett. , 62, 2146 (2008).
[16] K. Liu, X.-G. Chen Evolution of microstructure and elevated-temperature properties with Mn addition in Al-Mn-Mg alloys. J. Mater. Res. , 32, 2585 (2017).
[17] S. Manasijevic, Z. Pavlovic-Acimovic, K. Raic, R. Radisa, V. Kvrgić Optimisation of cast pistons made of Al–Si piston alloy. Int. J. Cast Met. Res. , 26, 255 (2013).
[18] L. Lodgaard, N. Ryum Precipitation of dispersoids containing Mn and/or Cr in Al–Mg–Si alloys. Mater. Sci. Eng., A, 283, 144 (2000).
[19] E. Cerri, E. Evangelista, S. Spigarelli, P. Cavaliere, F. DeRiccardis Effects of thermal treatments on microstructure and mechanical properties in a thixocast 319 aluminum alloy. Mater. Sci. Eng., A, 284, 254 (2000).
[20] A. M. F. Muggerud, E. A. Mørtsell, Y. Li, R. Holmestad Dispersoid strengthening in AA3xxx alloys with varying Mn and Si content during annealing at low temperatures. Mater. Sci. Eng., A, 567, 21 (2013).
[21] F. Stadler, H. Antrekowitsch, W. Fragner, H. Kaufmann, P. J. Uggowitzer: The Influence of Solution Treatment on the High-Temperature Strength of Al-Si Foundry Alloys with Ni. In: Suarez CE, editor. Light Metals 2012. Cham: Springer International Publishing; 2016. pp. 431.

Table

Table I Chemical composition of experimental alloys used (wt. %)

Alloy	Si	Fe	Cu	Mg	Ni	Mn	P	Al
A (base)	13.16	0.34	1.28	1.08	1.05	**0.02**	0.001	Bal.
M5	13.36	0.35	1.24	1.13	1.03	**0.53**	0.001	Bal.

Figures

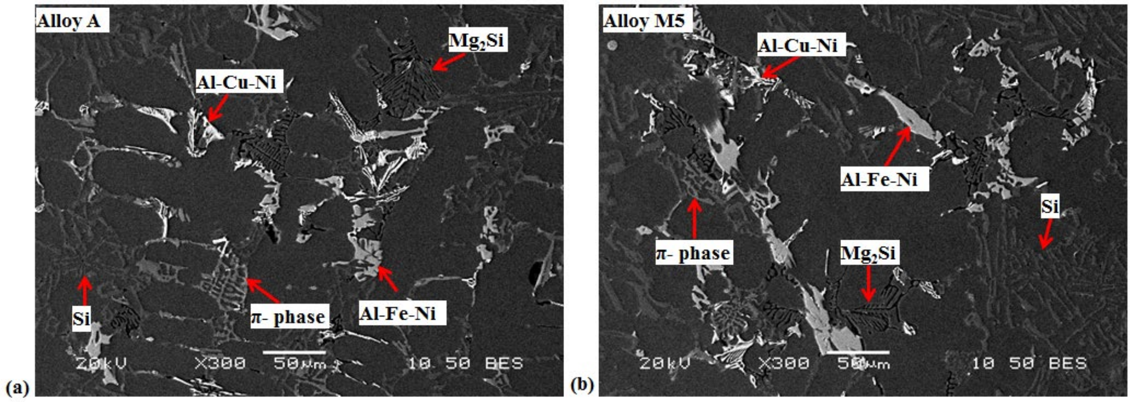

Fig. 1 Backscatter SEM images showing as-cast microstructure of experimental alloys: (a) Alloy A and (b) Alloy M5

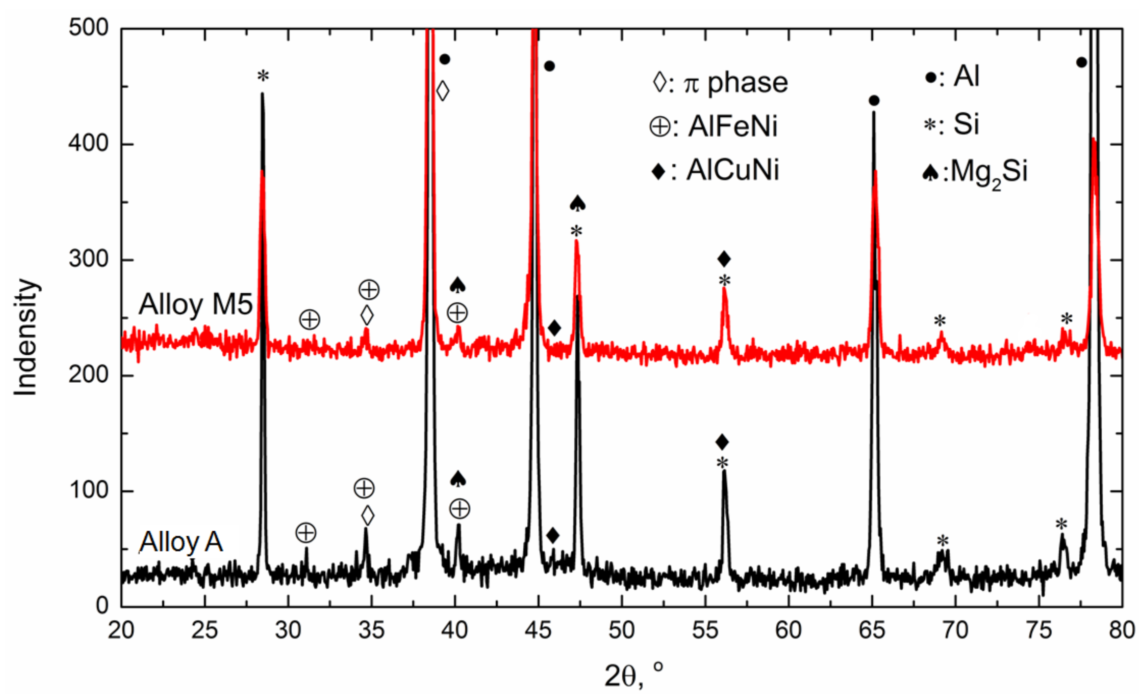

Fig. 2 XRD results of two experimental alloys in as-cast condition

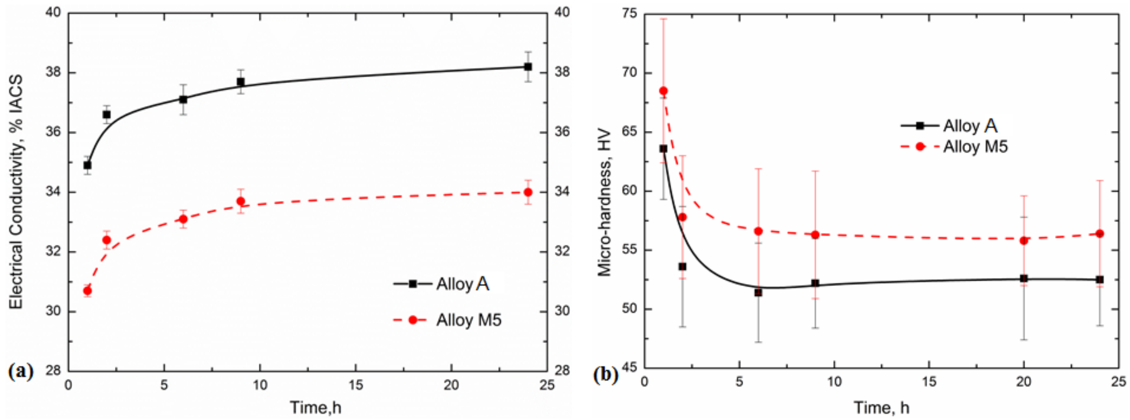

Fig. 3 Evolution of EC and microhardness during heat treatment at 375 °C: (a) EC and (b) microhardness

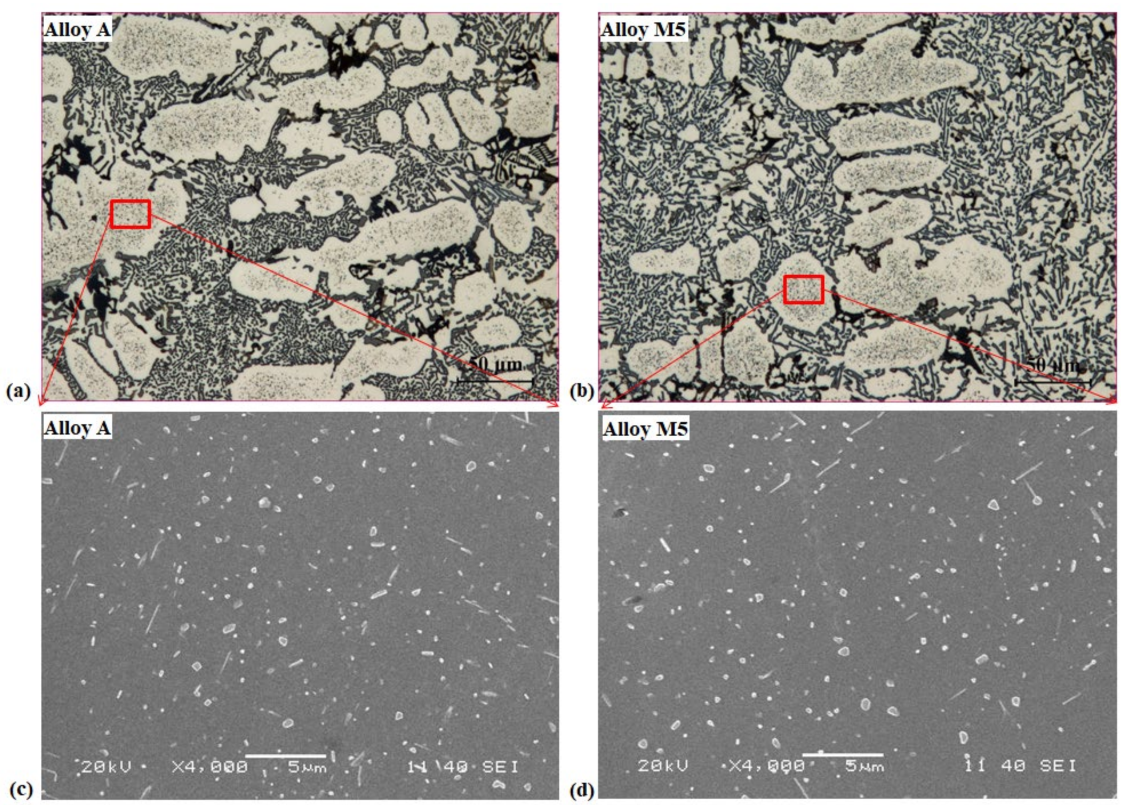

Fig. 4 Optical (a-b) and SEM (c-d) observation on the microstructure after 375°C/24h: (a) and (c) for Alloy A, (b) and (d) for Alloy M5

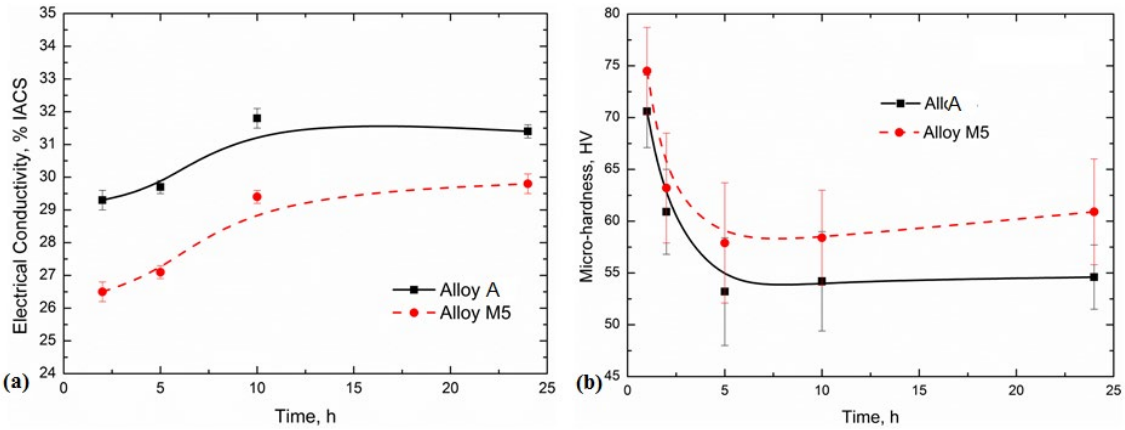

Fig. 5 Evolution of EC and microhardness during heat treatment at 425 °C: (a) EC and (b) microhardness

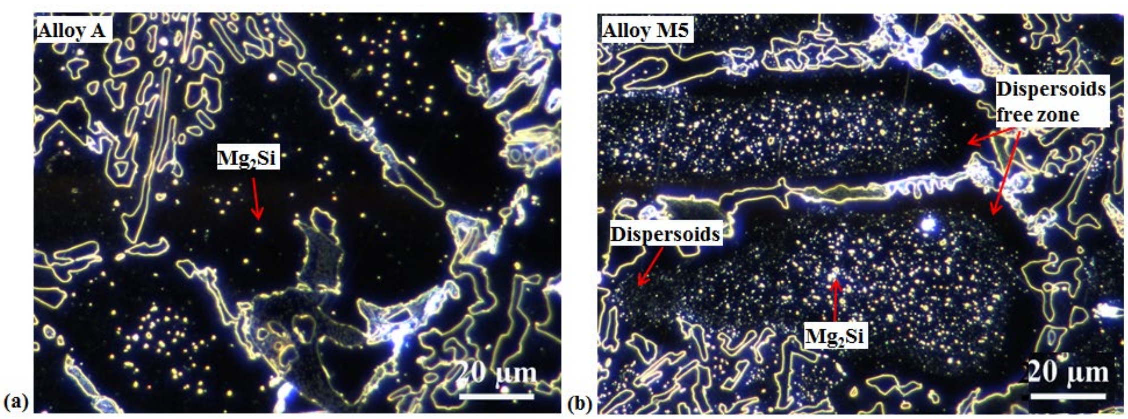

Fig. 6 Dark-field OM microstructure of experimental alloys after 425°C/24h: (a) Alloy A and (b) Alloy M5

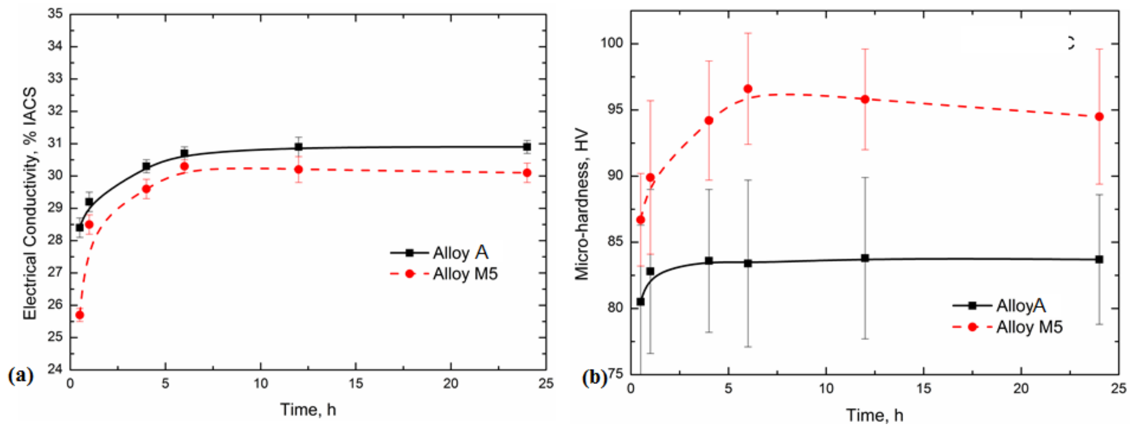

Fig. 7 Evolution of EC and microhardness during heat treatment at 500 °C: (a) EC and (b) microhardness

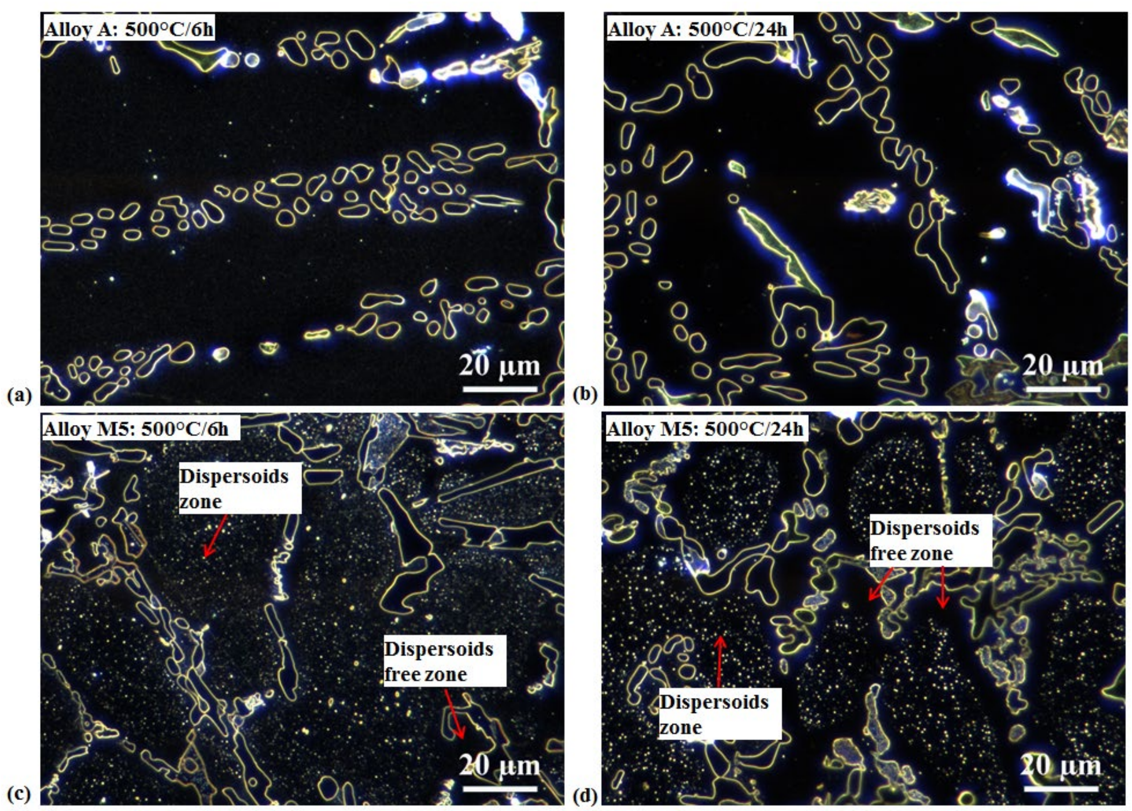

Fig. 8 Dark-field OM microstructure of experimetal alloys after treated at 500 °C: (a) Alloy A: 6h and (b) Alloy A: 24h; (c) Alloy M5: 6h and (d) Alloy M5: 24h

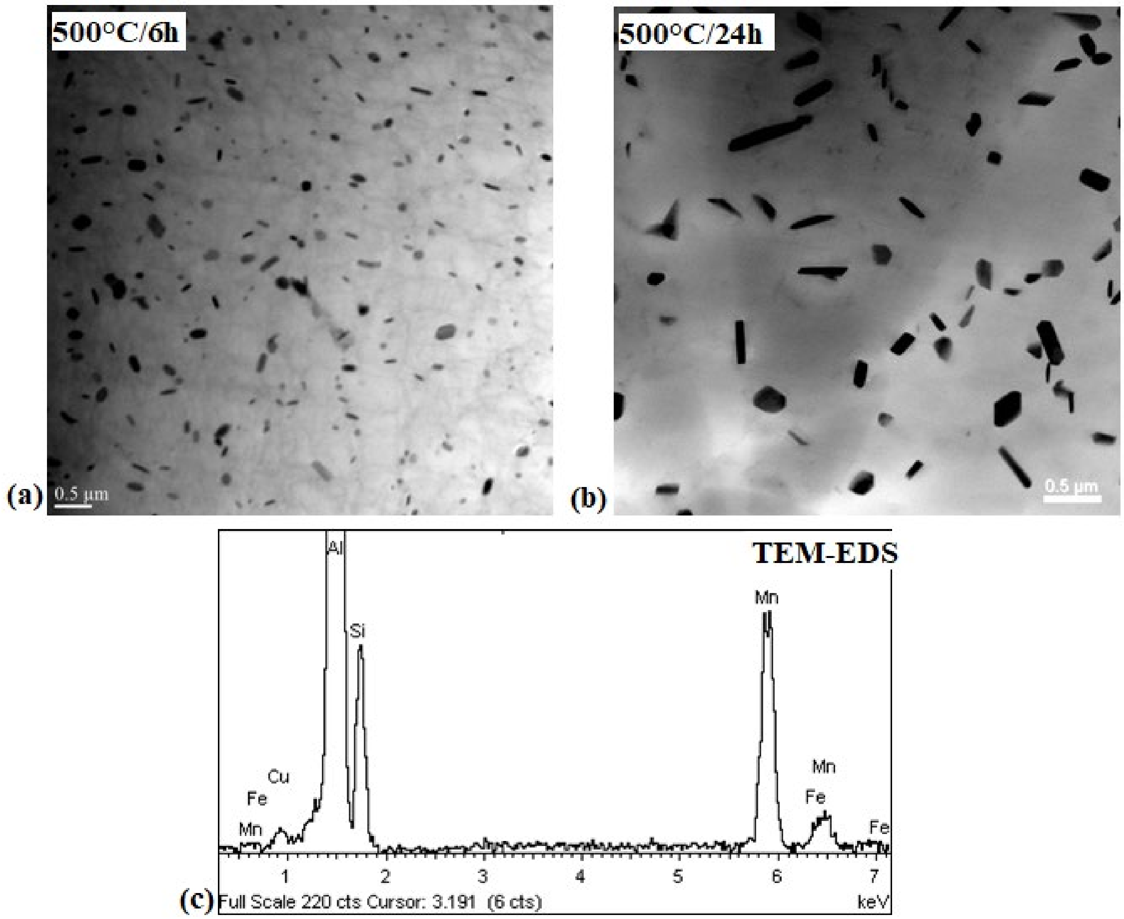

Fig. 9 TEM images showing the distribution of dispersoids in Alloy M5: (a) 500°C/6h, (b) 500°C/24h and (c) their TEM-EDS result

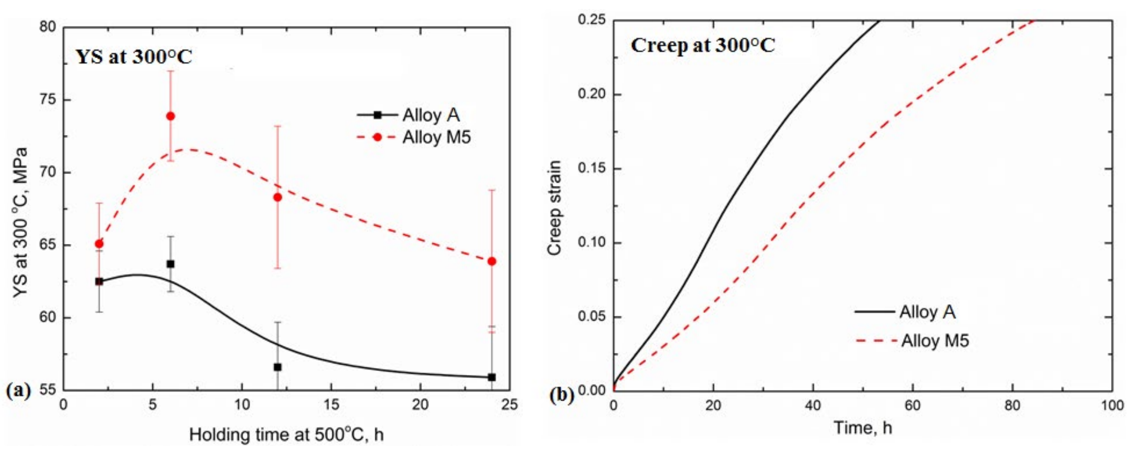

Fig. 10 Evolution of properties at 300 °C of experimental alloys : (a) YS as a function of holding time at 500 °C and (b) typical creep curves after 500°C/6h